



HAL
open science

National estimation of soil organic carbon storage potential for arable soils: A data-driven approach coupled with carbon-landscape zones

Songchao Chen, Dominique Arrouays, Denis Angers, Claire Chenu, Pierre Barré, Manuel Martin, Nicolas Saby, Christian Walter

► To cite this version:

Songchao Chen, Dominique Arrouays, Denis Angers, Claire Chenu, Pierre Barré, et al.. National estimation of soil organic carbon storage potential for arable soils: A data-driven approach coupled with carbon-landscape zones. *Science of the Total Environment*, 2019, 666, pp.355-367. 10.1016/j.scitotenv.2019.02.249 . hal-02051584

HAL Id: hal-02051584

<https://hal.science/hal-02051584>

Submitted on 22 Oct 2021

HAL is a multi-disciplinary open access archive for the deposit and dissemination of scientific research documents, whether they are published or not. The documents may come from teaching and research institutions in France or abroad, or from public or private research centers.

L'archive ouverte pluridisciplinaire **HAL**, est destinée au dépôt et à la diffusion de documents scientifiques de niveau recherche, publiés ou non, émanant des établissements d'enseignement et de recherche français ou étrangers, des laboratoires publics ou privés.



Distributed under a Creative Commons Attribution - NonCommercial 4.0 International License

Title: National estimation of soil organic carbon storage potential for arable soils: a data-driven approach coupled with carbon-landscape zones

Authors:

Songchao Chen ^{a, b}. songchao.chen@inra.fr

Dominique Arrouays ^a. dominique.arrouays@inra.fr

Denis A. Angers ^c. denis.angers@canada.ca

Claire Chenu ^d. claire.chenu@inra.fr

Pierre Barré, ^e. barre@geologie.ens.fr

Manuel P. Martin ^a. manuel.martin@inra.fr

Nicolas P.A. Saby ^a. nicolas.saby@inra.fr

Christian Walter ^b. christian.walter@agrocampus-ouest.fr

Affiliations:

^a INRA, Unité InfoSol, 45075 Orléans, France

^b UMR SAS, INRA, Agrocampus Ouest, 35042 Rennes, France

^c Québec Research and Development Centre, Agriculture and Agri-Food Canada, Québec, G1V 2J3 Canada

^d UMR Ecosys, INRA, AgroParisTech, Université Paris-Saclay, Campus AgroParisTech, 78850 Thiverval-Grignon, France

^e Laboratoire de Géologie de l'ENS, PSL Research University, UMR8538 du CNRS, 75231 Paris, France

Corresponding author: Songchao Chen

E-mail: songchao.chen@inra.fr

Telephone: +33(0)602142667

1 **Abstract**

2 Soil organic carbon (SOC) is important for its contributions to agricultural
3 production, food security, and ecosystem services. Increasing SOC stocks
4 can contribute to mitigate climate change by transferring atmospheric CO₂
5 into long-lived soil carbon pools. The launch of the 4 per 1000 initiative has
6 resulted in an increased interest in developing methods to quantify the
7 additional SOC that can be stored in soil under different management options.
8 We made a first attempt to estimate SOC storage potential of arable soils
9 using a data-driven approach based on the French National Soil Monitoring
10 Network. The data-driven approach was used to determine the highest
11 reachable SOC stocks of arable soils for France. We first defined different
12 carbon-landscape zones (CLZs) using clustering analysis. We then computed
13 estimates of the highest possible values using percentile of 0.8, 0.85, 0.9 and
14 0.95 of the measured SOC stocks within these CLZs. The SOC storage
15 potential was calculated as the difference between the highest reachable
16 SOC stocks and current SOC stocks for topsoil and subsoil. The percentile
17 used to determine highest possible SOC had a large influence on the
18 estimates of French national SOC storage potential. When the percentile
19 increased from 0.8 to 0.95, the national SOC storage potential increased by
20 two to three-fold, from 336 to 1020 Mt for topsoil and from 165 to 433 Mt for
21 subsoil, suggesting a high sensitivity of this approach to the selected
22 percentile. Nevertheless, we argue that this approach can offer advantages

23 from an operational point of view, as it enables to set targets of SOC storage
24 taking into account both policy makers' and farmers' considerations about
25 their feasibility. Robustness of the estimates should be further assessed using
26 complementary approaches such as mechanistic modelling.

27 **Keywords:** Soil organic carbon; Storage potential; Data-driven approach;
28 Carbon-landscape zones; Gaussian mixture models; Soil management
29 practices.

30 **1. Introduction**

31 Globally, the soil C pool (2500 Gt) is 3.3 times the size of the atmospheric
32 pool (760 Gt) and 4.5 times the size of the above-ground vegetation pool (560
33 Gt). Therefore, soils have the potential to partly offset anthropogenic
34 greenhouse gas emissions by sequestering SOC (Lal, 2004; Paustian et al.,
35 2016). Moreover, increasing soil organic carbon (SOC) generally improves
36 soil quality and functioning, and thus can potentially contribute to enhance
37 agricultural production and food security, restore degraded land, and promote
38 ecosystem services such as erosion mitigation, soil water provision, nutrient
39 availability for plants, and soil biodiversity (Lal, 2004; Stockmann et al., 2013).
40 Recognizing the importance of increasing SOC at the global scale, a voluntary
41 action initiative “4 per 1000 carbon sequestration in soils for food security and
42 the climate” (<http://4p1000.org/>) was launched at the COP21. The 4 per 1000
43 initiative aims at promoting land management practices (e.g., conservation
44 agriculture, cover cropping, agroforestry) leading to an increase in SOC
45 stocks in the 0 to 0.4m layer at an aspirational annual growth rate of 0.4% of
46 current SOC stocks (Lal, 2016; Minasny et al., 2017).

47 The SOC storage potential generally refers to the maximum gain in SOC
48 stock attainable at a given timeline by implementing changes in land use or
49 management, and will vary under different pedoclimatic conditions (Post and
50 Kwon, 2000; Stockmann et al., 2013; Barré et al., 2017; Chenu et al., 2018).
51 The concept of SOC saturation has been used to estimate the maximum

52 amount of SOC that can be associated with the fine fraction (Hassink, 1997)
53 and therefore considered as relatively stable. In the context of the 4 per 1000
54 initiative, the aspirational target of increasing SOC stocks at an annual growth
55 rate of 0.4% relates to the total (whole-soil) SOC stocks in the 0-0.4 m layer
56 (whole-soil, including the coarse fraction). Therefore, determining whole-soil
57 SOC storage potential using the maximum SOC associated with the fine
58 fraction is not appropriate because the SOC stored in the coarse fraction can
59 represent a large percentage of the total SOC stocks. As summarized by
60 Chen et al. (2018), under temperate climate, SOC in the coarse fraction could
61 account, on average, for 15%, 34% and 31% of total SOC stocks under
62 cropland, forest and grassland, respectively, in topsoil, and account for nearly
63 25%, 14% and 7% of SOC stocks for cropland, forest and grassland in subsoil.

64 For an improved quantification of SOC storage potential, Barré et al. (2017)
65 proposed one avenue: i) First, establish the reference stocks with an estimate
66 of the highest reachable SOC stock for a given soil; ii) second estimate
67 possible SOC storage between the current SOC stock of a given soil and this
68 reachable highest SOC stock under a given land-use for different land
69 management practices. Furthermore, Barré et al. (2017) suggested that this
70 avenue can be achieved using either a data-driven approach (empirical
71 observation of SOC stocks and storage) or mechanistic simulation models.
72 The data-driven approach assumes that the highest reachable SOC stocks
73 under a specific land use/cover or land management practices for each

74 different pedoclimatic conditions could be empirically determined by the
75 highest values (e.g., by the mean of using top quantiles) among the observed
76 SOC stocks for these conditions. This hypothesis implicitly assumes that the
77 values of the top quantiles reflect the optimal management practices for SOC
78 storage and they are thus considered as ‘proxies’ of the maximum reachable
79 SOC stocks under these different pedoclimatic conditions.

80 Based on the detailed and extensive French Soil Monitoring Soil Network
81 data base, our objective was to test a data-driven approach for estimating
82 SOC storage of arable soils in mainland France. We developed a procedure
83 which consisted of: i) determining carbon-landscape zones by clustering the
84 data from a combination of net primary production (C input), climatic
85 decomposition index (C decomposition) and soil clay content (C protection
86 from decomposition); ii) estimating the maximum SOC stocks of arable soils
87 (topsoil and subsoil) for each carbon-landscape zone using four percentiles
88 (0.80, 0.85, 0.90 and 0.95); iii) calculating by difference with the current SOC
89 stocks, the SOC storage potential of arable topsoil and subsoil under these
90 four percentiles.

91 **2. Materials and methods**

92 2.1 Soil data

93 Covering the entire mainland France under different soil, climate, relief and
94 land cover conditions, 2092 sites from the first campaign of the French Soil

95 Monitoring Network (RMQS) were sampled from 2001 to 2009. The RMQS is
96 based on a 16 km × 16 km square grid and all sites were selected at the
97 centre of each grid cell. Topsoil (0-30 cm) and subsoil (30-50 cm) were
98 collected using a hand auger. For each site, 25 samples were merged into a
99 composite sample and then were air-dried (controlled at a temperature of 30
100 °C and an air-moisture of 30%) and sieved to 2 mm before laboratory analysis.
101 A soil pit was dug at 5 m from the south border of sampling sites, and the
102 main soil characteristics were recorded and bulk density and percentage of
103 coarse elements were measured (Martin et al., 2009). For some RMQS sites,
104 subsoil did not exist as soils were thin at these locations. SOC was
105 determined by dry combustion. Only these RMQS sites (n=1089) located on
106 arable soils were used in this study (Figure 1).

107 The SOC stock was calculated as below:

$$SOC_{stock} = p \times SOC \times BD \times (100 - ce) \times 10^{-2} \quad (1)$$

108 where SOC_{stock} is the SOC stock (kg m^{-2}), p is the actual thickness (cm) of
109 topsoil or subsoil, SOC , BD and ce are the content of SOC (g kg^{-1} or ‰), bulk
110 density (kg m^{-3}), and percentage of coarse elements (%).

111 2.2 Net primary production, climatic data, soil clay content and SOC stocks
112 maps

113 Net primary production (NPP) was extracted from the MOD17A2H version
114 6 Gross Primary Production product (NASA LP DAAC, 2017) from 2000 to

115 2010. It is a cumulative 8-day composite of values with 500-meter original
116 resolution. The 8-day NPP data is averaged into monthly data and resampled
117 to 1 km resolution. Cities and water-covered regions have been masked in
118 this product.

119 WorldClim Version 2 (Fick and Hijmans, 2017), which is spatially
120 interpolated using between 9000 and 60000 weather stations globally, was
121 used for climatic data: It has average monthly climate data for minimum,
122 mean, and maximum temperature and for precipitation, solar radiation, wind
123 speed and water vapour pressure for 1970-2000 at 1 km resolution.

124 Maps of soil clay content for topsoil (0-30 cm) and subsoil (30-50 cm) were
125 derived from *GlobalSoilMap* France products (Mulder et al., 2016). As these
126 were produced at six standard depth intervals (e.g., 0-5 cm, 5-15 cm, 15-30
127 cm, 30-60 cm, 60-100 cm and 100-200 cm), soil clay content maps were
128 harmonized using a depth-weighted method (Appendix Figure A1).

129 The Corine Land Cover 2006 (UE-SOeS, 2006) was used as the land
130 cover/use classification map. It has an original resolution at 100 m and was
131 resampled to 90 m in order to meet the requirement of the *GlobalSoilMap*
132 project (Sanchez et al., 2009; Arrouays et al., 2014). The Corine Land Cover
133 map was reclassified as cropland, forest, grassland and others, and only
134 cropland was presented in this study (Figure 1).

135 The current SOC stocks map for topsoil (0-30 cm) was produced using
136 RMQS dataset by a hybrid model coupling the boosted regression trees (BRT)

137 and robust geostatistical approaches described in Martin et al. (2014). The
138 covariates used in modelling were explicitly documented in Chen et al. (2018).
139 To remove the interference of the positions without SOC stocks in subsoils
140 (where subsoil does not exist), a three-stage approach was applied for SOC
141 stocks modelling in the subsoil (30-50 cm): 1) produce a map to identify
142 whether subsoils exist using BRT model; 2) produce a SOC stocks map by
143 the hybrid model, where the RMQS sites without SOC stocks are excluded; 3)
144 merge the two maps by keeping the SOC stock values where subsoils exist
145 and setting the locations where subsoil do not exist as NA (not available). The
146 SOC stocks maps for topsoil and subsoil have a spatial resolution of 90 m and
147 they can be found in the Appendix Figure A2. The national SOC stocks were
148 3.65 Gt and 1.04 Gt for topsoil and subsoil, respectively. Cropland contained
149 1.37 Gt and 0.44 Gt SOC in the topsoil and subsoil.

150 All the datasets were reprojected to Lambert 93, which is an official
151 projection for mainland France.

152 2.3 Calculation of climatic decomposition index

153 Carbon decomposition generally increases with temperature and moisture,
154 a climatic decomposition index (CDI) was used to characterise the interaction
155 between temperature and water stress as suggested by Carol Adair et al.
156 (2008).

157 Before determining the CDI, potential evapotranspiration (PET) was
158 calculated using Hargreaves model (Hargreaves et al., 1985), which performs

159 well and requires less parameterization than the Penman-Monteith method
160 (Hargreaves and Allen, 2003). Monthly PET (mm month^{-1}) is defined below:

$$PET = 0.0023 \times SR \times (T_{mean} + 17.8) \times \sqrt{T_{range}} \quad (2)$$

161 where SR is monthly solar radiation (mm month^{-1} , transformed from KJ m^{-2}
162 day^{-1}), T_{mean} is monthly mean temperature ($^{\circ}\text{C}$) and T_{range} is the difference
163 between the monthly maximum and minimum temperature ($^{\circ}\text{C}$).

164 The CDI is calculated as a function of the mean monthly mean
165 temperature (T), monthly precipitation (PPT) and monthly PET (Carol Adair et
166 al., 2008):

$$CDI = F_T(T) \times F_W(PPT, PET) \quad (3)$$

$$F_T(T) = 0.5766 \times e^{308.56 \times \left(\frac{1}{56.02} - \frac{1}{(273+T)-227.13} \right)} \quad (4)$$

$$F_W(PPT, PET) = \frac{1}{1 + 30 \times e^{-8.5 \times \frac{PPT}{PET}}} \quad (5)$$

167 where $F_T(T)$ and $F_W(PPT, PET)$ are the monthly effects of temperature and
168 water stress on decomposition.

169 2.4 Delineation of carbon-landscape zones using Gaussian mixture models

170 Generally, SOC dynamics depend on the trade-off between the SOC input
171 and SOC loss processes. When SOC input is greater than OC loss, the soil
172 will accumulate C, and otherwise, soil C will decrease (Lal et al., 2015).
173 Climatic decomposition index and NPP are here considered as proxies of C
174 loss and input that control the SOC balance, and clay content considered as a
175 controlling factor of SOC persistence. The underlying simplifying assumption
176 is that decomposition mainly depends on both climate and soil characteristics.

177 Therefore monthly CDI and NPP, and soil clay content were used to compute
178 the carbon-landscape zones (CLZs) using Gaussian mixture model (GMM)
179 which is a similar approach to that used by Mulder et al. (2015). To reduce
180 multicollinearity and computing time, principal component analysis (PCA) was
181 performed before the clustering step on monthly CDI and NPP data separately.
182 We retained only the first three and four principal components that explained
183 more than 95% of the variance for CDI and NPP, respectively. Therefore, after
184 adding soil clay content for topsoil and subsoil, a total of nine variables were
185 used for GMM clustering. Moreover, to reduce computing complexity, we also
186 selected 20000 pixels in France as calibration data set of the GMM clustering.
187 The resulting clustering model was then used to predict to which CLZ each
188 pixel of the entire territory belongs.

189 Gaussian mixture model was conducted to compute clusters that were
190 considered as CLZs in this study. GMM is one of the model-based clustering
191 techniques, which optimizes the fit between the measured data and
192 mathematical models using a probabilistic approach. GMM is based on the
193 assumption that the data are generated by a mixture of Gaussian distributions.
194 Then, the parameters of GMMs are estimated by maximisation of the
195 likelihood using the Expectation Maximization (EM) algorithm. EM algorithm
196 starts with a random initialization and then iteratively optimizes the clustering
197 using two steps: (i) Expectation step determines the expected probability of
198 assignment of data to clusters using current model parameters; (ii)

199 Maximisation step updates the optimal model parameters of each mixture
200 based on the new data assignment.

201 The number of clusters was tuned from 1 to 30 and their associated
202 Bayesian information criterion (BIC) was calculated for the evaluation of
203 clustering performance. The number of clusters was selected considering a
204 trade-off between the BIC values and the available number of RMQS sites
205 within each land use for each cluster. GMMs were performed using ClusterR
206 package in R 3.3.2 (Mouselimis, 2016; R Core Team, 2016). The optimized
207 CLZs map was resampled to 90 m resolution.

208 2.5 SOC storage potential and analysis of the sensitivity to the percentile
209 setting

210 Empirical maximum SOC stock values were estimated for arable topsoil
211 and subsoil under given CLZs using RMQS dataset (point observations). Four
212 percentiles at 80%, 85%, 90% and 95% were tested to estimate the empirical
213 maximum SOC stock values that could be reached under a given CLZ. A
214 bootstrapping approach was applied to assess the uncertainty from data
215 source both for each CLZ and tested percentiles. We repeated the
216 bootstrapping procedure 100 times and thus obtained 100 estimates of the
217 maximum SOC stock values for each CLZ and percentile. The mean value
218 obtained from these one hundred estimates was used as an estimate of the
219 maximum SOC stock value for each CLZ and percentile. We then estimated
220 the uncertainty (90% confidence intervals, 90% CIs) of these maximum SOC

221 stock values by using the 5 and 95 percentile of the bootstrapping results.

222 The SOC storage potential was calculated as the difference between the
223 empirically-determined maximum SOC stocks and current SOC stocks (Figure
224 A2) under arable land use. Four SOC storage potential maps were produced
225 using the four tested percentiles for both topsoil and subsoil, and their
226 associated 90% CIs.

227 We evaluated the effect of percentile setting on the estimation of SOC
228 storage potential by both comparing the differences in the SOC storage
229 potential spatial distribution and national SOC storage potential estimates.

230 **3. Results**

231 3.1 Spatial distribution of CDI, NPP and their principal components

232 Figure 2 shows the spatial distribution of CDI and NPP in mainland France.
233 Globally, CDI increased gradually from January to August and then decreased
234 gradually to December. Different from CDI, NPP started to increase from
235 January and reached the peak in June, and then decreased gradually to
236 December.

237 Accounting for 98.3% and 97.0% of the total variances (95% was set as a
238 threshold), the first three and four principal components (PCs) were kept for
239 CDI and NPP, respectively. Figure 3 presents the final seven PCs used in
240 clustering. The 3 PCs of CDI showed long range spatial patterns in mainland
241 France while the spatial patterns for 4 PCs of NPP were mainly characterized

242 by median and short ranges.

243 3.2 Carbon-landscape zones

244 The BIC value decreased quickly when the number of clusters was less
245 than 10, and then it decreased slowly after 10 clusters (Figure 4). The result
246 indicated that more clusters were helpful for separating the differences within
247 clusters. However, more clusters meant less available RMQS sites falling into
248 each cluster. Figure 5 shows the number of RMQS sites located in each
249 cluster. Our aim was to avoid clusters having a number of RMQS sites less
250 than ten, which may not be enough to derive a robust estimate of the
251 quantiles. Two clusters had less than ten RMQS sites when the number of
252 clusters varied from 8 to 10. When the number of clusters increased from 11
253 to 13, three clusters were found with less than ten RMQS sites. We optimized
254 the number of clusters at ten as it appeared to be the best compromise
255 between separating the differences between clusters and keeping an
256 acceptable number of clusters having less than ten RMQS sites.

257 Figure 6 illustrates the spatial distribution of CLZs in mainland France.
258 CLZ 1 is mainly distributed in north-eastern France which is characterized by
259 a rather continental climate and relatively high soil clay contents, mostly
260 ranging from 22% to 35% in topsoil, and being even higher in subsoil
261 (Appendix Figure A3). CLZ 2 represents most of western France
262 characterized by a mild and wet oceanic climate and relatively homogeneous
263 soil clay contents (mostly ranging from 15 to 20% both in top- and subsoil,

264 Appendix Figure A3). CLZ 3 is located in northern France and mainly
265 corresponds to the maximal extension of deep loess deposits. It exhibits clay
266 contents centred around 20% for topsoil and a bit higher for subsoil, both with
267 a rather low statistical dispersion. CLZ 4 is located in the Massif Central and
268 the Vosges mountains, and is characterized by a rather cold climate due to
269 elevation and rather homogeneous clay contents, mostly ranging from 15% to
270 20% for both layers (Appendix Figure A3). CLZ 5 is located in southern
271 France and strictly corresponds to the area of the 'Landes of Gascony' which
272 is characterized by a mild climate and nearly pure sandy aeolian deposits
273 having clay content nearly always less than 5% (Augusto et al., 2010). CLZ 6
274 is located in central France and corresponds to the foothills of the Massif
275 Central, with a lower elevation than its central part. Part of the CLZ 6 is also
276 spread in various other locations, all of which corresponding to ancient alluvial
277 deposits coming from these foothills. In topsoil, most clay contents range from
278 15% to 20% and slightly higher in subsoil. CLZ 7 is exclusively located in the
279 highest elevations located at the top of the main mountain ranges (Pyrenees,
280 Alps, Jura and Massif Central), with soil texture being rather clayey (around
281 30%). This CLZ also includes many thin soils (Lacoste et al., 2016), and thus
282 the information on clay content of the 0.3 to 0.5 m layer is often missing. CLZ
283 8 occupies most of south-western France characterized by mild winters and
284 hot summers. It is characterized by a very large range and dispersion of clay
285 content in both layers, although a large part (interquartile range) ranges from

286 20% to 30%. CLZ 9 is mainly distributed in central and northern France. Its
287 clay content in topsoil and subsoil is centred around 25% (Appendix Figure A3)
288 and showing a small increase in subsoil. Lastly, CLZ 10 shows low NPP
289 values in autumn, because of land use consisting mainly of vineyards and
290 wheat crops. It is clearly located in the Mediterranean region with very hot
291 temperatures and very low NPP in summer. The clay content is centred
292 around 20%, with a statistical dispersion similar to the other CLZs.

293 Figure 7 presents the design-based estimates of SOC stocks for arable
294 soils for the ten CLZs in topsoil and subsoil. In order to get unbiased
295 estimates, these estimates were computed using the values obtained from the
296 RMQS grid values within each CLZ. The median SOC stocks of topsoil
297 ranged from 4.89 to 9.67 kg m⁻² under the 10 CLZs. Fewer differences of SOC
298 stocks were found in subsoil, and subsoil had much lower SOC stocks than
299 topsoil with a range of median SOC stocks from 1.31 to 2.08 kg m⁻².

300 3.3 Empirical maximum SOC stocks under four percentile settings

301 As expected, there was a clear trend that the maximum SOC stocks for
302 topsoil and subsoil increased when percentile became higher, however, the
303 magnitude of these increases varied among different CLZs (Figure 8). In
304 topsoil, large differences (>4 kg m⁻²) in maximum SOC stocks between
305 percentile of 0.95 and percentile of 0.8 were observed in CLZ 1 and CLZ 4,
306 and the differences ranged from 0.28 to 3.65 kg m⁻² for other CLZs. In subsoil,
307 differences in maximum SOC stocks between percentile of 0.95 and

308 percentile of 0.8 were below 1.5 kg m^{-2} for almost all the CLZs, except for CLZ
309 4 with a value of 2.71 kg m^{-2} .

310 The 90% CIs also differed between CLZs as well as between percentiles.
311 A large percentage of high 90% CIs (upper limit minus lower limit $> 10 \text{ kg m}^{-2}$
312 for topsoil or $> 5 \text{ kg m}^{-2}$ for subsoil) of maximum SOC stocks were found in
313 CLZ 4 and CLZ 7, which indicated large variability for these two mountainous
314 CLZs having a rather low number of sites. Besides, subsoil in arable soils had
315 lower 90% CIs than topsoil.

316 3.4 Spatial distributions of SOC storage potential

317 Figure 9 and Figure 10 show the spatial distributions of SOC storage
318 potential and 90% CIs under four percentile settings for topsoil and subsoil,
319 respectively. When percentile was set at 0.8, French arable topsoil had a SOC
320 storage potential less than 2 kg m^{-2} except for a part of Brittany and south-
321 eastern France near the Mediterranean Sea. With the increasing percentile,
322 intensively cultivated plains of the central, the northern half and the
323 southwestern part of France showed a large potential to store more SOC.
324 Cropland located around mountainous regions including the Pyrenees, the
325 Alps, the Jura and the Vosges generally had a relatively low SOC storage
326 potential across all percentiles. Large differences were observed for total SOC
327 storage potential under different percentile settings (Table 2). The French
328 national SOC storage potential and 90% CIs for arable topsoil were 336
329 (203,501) Mt when percentile was 0.8. Larger increases were observed for

330 total SOC storage potential and 90% CIs with the increasing percentiles,
331 which reached at 470 (308,662) Mt, 674 (434,950) Mt and 1020 (740,1283) Mt
332 for a percentile of 0.85, 0.9 and 0.95, respectively.

333 The subsoil showed much lower SOC storage potential than topsoil. Most
334 regions of mainland France had low SOC storage potential ($< 1 \text{ kg m}^{-2}$) at
335 percentiles of 0.8 and 0.85, and relative high SOC storage potential ($1\text{-}3 \text{ kg m}^{-2}$)
336 were observed in central France. Similar with topsoil, increasing percentiles
337 resulted in higher SOC storage potential across mainland France, and fewer
338 differences of SOC storage potential were found between cropland located
339 around mountainous regions and other regions under four percentile settings.
340 At percentile of 0.8, subsoil had the potential to sequester 165 Mt additional
341 SOC with a 90% CI between 91 Mt and 250 Mt. Total SOC storage potential
342 and their 90% CIs were 228 (150,306) Mt, 309 (226,404) Mt and 433 (331,560)
343 Mt for percentiles of 0.85, 0.9 and 0.95, respectively.

344 **4. Discussion**

345 4.1 Optimizing and mapping Carbon Landscape Zones

346 The estimates of SOC storage potential using a data-driven approach
347 were based on a stratification of the study area using the CLZs, therefore a
348 procedure for optimizing the number of CLZs was necessary. We observed a
349 negative trend between the number of clusters and BIC, which indicated that
350 using more clusters allowed to explain more variance of our covariates.

351 However, as soil data was finite, creating too many clusters would have
352 resulted in fewer soil data available for each CLZ. We assumed in this study
353 that performing a statistical analysis with less than 10 samples was not robust;
354 therefore we decided to optimize the number of clusters by considering a
355 trade-off between the BIC value and the number of RMQS sites located within
356 each cluster. Interestingly, though using a very different set of covariates and
357 soil point data (different covariates, and a much larger number of soil point
358 data), Mulder et al. (2015) found that the same number of clusters (10) was
359 optimal to partition points data into soil-landscape systems relevant to SOC.
360 Moreover, their maps showed rather similar spatial patterns (e.g. in the
361 Mediterranean region, mountains, and western France).

362 4.2 National SOC storage potential

363 As expected, the percentile setting had a strong influence on the
364 estimation of SOC storage potential (Table 2). If we use the national SOC
365 storage potential at a percentile of 0.8 as a benchmark, the total SOC storage
366 potential at percentiles of 0.85, 0.9 and 0.95 were 1.40, 2.01 and 3.04 times
367 larger, respectively, in topsoil and were 1.38, 1.87 and 2.62 times larger,
368 respectively, in the subsoil. Clearly, the estimates of SOC storage potential
369 are very sensitive to the percentile chosen, especially at high values setting
370 (e.g., 0.95).

371 4.3 Limitations of the data-driven approach

372 The data-driven approach has previously been implemented in a few
373 pedoclimatic regions to estimate SOC storage potential. Stolbovoy and
374 Montanarella (2008) used data from the European Soil Portal database to
375 determine the maximum observed SOC stocks for a given soil type under a
376 given climate, from which they subtracted the observed SOC stocks under
377 cultivated land. Lilly and Baggaley (2013) determined for each typological soil
378 unit the observed maximum SOC stocks, from which they subtracted the
379 observed median SOC stock under cultivated topsoils. One main difference
380 between these studies and the present one is that they did not calculate
381 percentiles but used only as reference the maximum observed values which
382 are obviously much more sensitive to the presence of very high values.
383 Another difference is that they used coarse resolution data, some of which
384 may not always be directly related to controlling factors of SOC (e.g., soil type,
385 highly aggregated data for delineating large bioclimatic regions).

386 We show here that this approach has some limitations. It is very sensitive
387 to percentile setting. This is partly attributable to the fact that the SOC
388 distributions are highly skewed with long tails at high SOC values (e.g., CLZs
389 1, 3, 4, 6, 8 and 10, see Fig.7 and Fig.8). This approach could be also
390 considered as data 'hungry'. This sensitivity is also linked to the fact that we
391 have a rather limited number of observations for some CLZs, especially those
392 with a small crop land area (e.g. CLZs, 4 and 7, see Fig. 8), which hampers
393 the robustness of the data-driven approach. Another limitation may come from

394 the fact that some cultivated soils may have been recently converted from
395 other land uses (e.g., grassland, forest) and may not have yet reached an
396 equilibrium level, which could partly explain the long tails that we observed.
397 One alternative approach would consist in performing dedicated sampling in
398 the CLZs following a probability sampling as suggested by De Gruitjer et al.
399 (2016). In this approach, the number of sites is selected with a minimum
400 number in order to get precise estimates of the quantiles.

401 In addition, Barré et al. (2017) already mentioned two other limitations.
402 Firstly, this approach provides an estimate of soil storage potential under
403 present management practices, therefore this estimate could be largely
404 underestimated when new SOC aggrading techniques are adopted. As
405 discussed by Sparling et al. (2003), current management practices may
406 strongly affect the outcomes of a data driven approach when deriving
407 desirable soil organic carbon contents from the median of observed SOC
408 contents. Secondly, another limit of data-driven approaches would be that, for
409 most available databases, management practices are not documented, and
410 thus make it difficult to determine their influence (Barré et al., 2017). Indeed,
411 in some cases there is still a large diversity of soils within a same CLZ and
412 also very different land use histories which are not considered in this
413 approach. The influence of these two factors on the potential storage maps
414 can be easily seen for instance for western France (CLZ2, characterized by a
415 gradient linked to the date of grasslands conversion to croplands). Similarly,

416 the gradients observed in piedmont areas may be linked to the fact that large
417 parts of them have been more or less recently converted from forest or
418 grassland to cropland (e.g., Arrouays et al., 1994, 1995a, 1995b; Saby et al.,
419 2008) and thus still have quite large SOC stocks reflecting their past land use.
420 Finally, a CLZ may include very different agricultural production systems and
421 in some cases reaching the storage potential would not only require to change
422 the management practices, but the whole production system. The estimates
423 we provide may be refined in the future taking into account the different
424 agricultural production systems (for CLZ with enough sites).

425 Despite these limitations, we consider that this first national approximation
426 of SOC storage potential is valuable in making use of a detailed and robust
427 nation-scale database. We further point out some operational advantages of
428 the data driven approach in section 4.6.

429 4.4 Complementarity with other approaches

430 Using a method based on the carbon saturation equation of Hassink
431 (1997), Chen et al. (2018) estimated the SOC sequestration potential in
432 mainland France using the same RMQS data. In their work, the concept of
433 SOC sequestration potential referred to the additional SOC associated with
434 soil fine fraction ($< 20 \mu\text{m}$), assumed to have pluri-decadal residence times.
435 Their results showed that arable topsoil and subsoil could theoretically
436 sequester 646 Mt and 752 Mt SOC, respectively. Though SOC associated
437 with the soil fine fraction does not represent the total SOC, their estimate of

438 SOC sequestration potential in arable topsoil was close to the percentile of
439 0.9 derived SOC storage potential (674 Mt), suggesting that SOC
440 sequestration potential can hardly be reached under current management
441 practices. The maps of SOC sequestration potential obtained applying
442 Hassink's equation (Chen et al., 2018) and the maps of SOC storage potential
443 obtained through the data driven approach show rather good qualitative
444 agreements in the western part of France. However, noticeable differences
445 are observed in mountain areas and in the most clayey CLZs for which the
446 data driven approach predicts a much lower additional storage potential than
447 the theoretical SOC sequestration potential. Apart from the fact that the two
448 maps rely on different concepts (sequestration and storage, e.g., Barré et al.,
449 2017; Chenu et al., 2018) and different modes of calculation, this may also
450 suggest that the pedoclimatic conditions in rather cold or clayey situations do
451 not allow to reach the theoretical SOC sequestration potential because of
452 insufficient plant biomass inputs. In arable subsoil, SOC storage potentials
453 derived from a data-driven approach (under all percentiles) were much lower
454 than C-saturation theoretical SOC sequestration potential. This may be
455 attributed to the fact that the present data-driven estimate of SOC storage
456 potential is based on current land management practices, while reaching the
457 estimated SOC sequestration potential for subsoil may need more advanced
458 land management practices with more potential to raise the SOC in both
459 topsoil and deeper layers (Chenu et al., 2018). This may be also simply due to

460 the fact that the French pedoclimatic conditions do not allow to reach the C-
461 saturation theoretical SOC sequestration potential.

462 As suggested by Barré et al. (2017), the model-driven approach would be
463 another way of estimating SOC storage potential. In a model-driven approach,
464 process-based models are used for determining highest reachable SOC
465 stocks by simulating different management scenarios. Such an approach has
466 been applied to EU by Lugato et al. (2014). Compared to a data-driven
467 approach, this process-based model may be more suitable as it is able to
468 monitor SOC stock dynamics. However, there are also some limitations to this
469 model-driven approach: i) a lot of input data is required for modelling, for
470 instance, a CENTURY model needs site-specific precipitation, temperature,
471 soil texture, bulk density, initial SOC, land use and corresponding
472 management practice; ii) the initialization for C dynamic models is still very
473 problematic and the simulation for large dataset is time-consuming; iii) the
474 accuracy of C dynamics model prediction needs to be validated by resampled
475 soil data and (iv) the soil management options considered are limited to those
476 accounted for in current SOC dynamics models (e.g. agroforestry may not be
477 considered in most models).

478 4.5 SOC storage potential and 4 per 1000 goal

479 Based on our current SOC stock maps shown in Figure A2, the total SOC
480 stocks are estimated at 1.37 Gt and 1.81 Gt for French arable soils for the 0-
481 30 cm layer and the 0-50 cm layer, respectively. If we base these estimates

482 on the total area of French arable soils, reaching the 4 per 1000 aspirational
483 target would require a storage rate of 5.48 Mt C year⁻¹ for 0-30 cm, or 7.24 Mt
484 C year⁻¹ for 0-50 cm. According to the C storage rate for 0-30 (0-50) cm, it
485 would take 61 (69), 85 (96), 122 (135) and 186 (200) years to reach the SOC
486 storage potential under percentiles of 0.8, 0.85, 0.9 and 0.95, respectively.
487 Thus our data-driven estimates of C storage potential suggest that achieving
488 an annual rate of increase of 0.4% would have to be maintained for decades
489 before reaching the SOC storage potential of these soils, provided that
490 relevant management options can be implemented for such an annual SOC
491 storage, and keeping in mind that an equilibrium level may be reached after a
492 few decades.

493 4.6 The data driven approach, a potentially operational tool

494 We observed that that SOC storage potential is very sensitive to the
495 percentile used in the calculation. We submit that this approach offers
496 potential for operational purposes as it enables to set targets of SOC carbon
497 storage for both policy makers and farmers. For instance, decision-makers
498 may decide to implement policies aiming at reaching a minimal objective (for
499 instance, all sites should reach the 0.6 percentile), an intermediate objective
500 (0.8 percentile) or an ambitious objective (0.9 percentile). It could therefore be
501 a very suitable tool to determine to which extent soils can contribute to
502 Intended Nationally Determined Contributions (INDCs). As an additional step,
503 more emphasis should be put both on policy and recommendations to reach

504 these objectives for different soils, agricultural productions systems and land
505 use histories within each CLZ, and ultimately on developing methods to verify
506 that the targeted objectives are reached. This approach could then be further
507 used to improve the data-driven approach and to design future objectives.
508 Similarly, at a local scale, farmers may compare their present SOC stocks to
509 the theoretically reachable ones within their CLZ, and decide which goal may
510 be reachable by implementing more or less drastic or costly changes to their
511 management practices. They may even find out that the SOC stocks at their
512 farm level are already close to the maximal reachable value, and thus
513 concentrate on not losing SOC rather than on trying to increase the current
514 stocks.

515 **5. Conclusions**

516 We tested a data-driven approach to estimate SOC storage potential
517 under Carbon Landscape Zones for arable soils using the French National
518 Soil Monitoring Network. Under the trade-off between the BIC index and
519 available data for robust statistics, the optimized number of CLZs was
520 determined at 10, using monthly NPP, CDI, and clay content data. The
521 national SOC storage potential varied from 336 Mt to 1020 Mt for topsoil and
522 from 165 Mt to 433 Mt for subsoil under four percentile settings (0.8, 0.85, 0.9
523 and 0.95), which shows that the data-driven approach is very sensitive to the
524 selected percentile. This sensitivity was partly attributable to a rather low
525 number of observations in some CLZs and mainly to skewed distributions with

526 long tails of high SOC contents. However, we argue that this data driven
527 approach offers meaningful advantages from an operational point of view, as
528 it enables to adapt targets of SOC carbon storage by taking into account both
529 policy makers' and farmers' considerations. We also argue that the data
530 driven approach is also a convenient way to provide quantitative estimates of
531 the SOC storage potential over large areas having widely distributed soil data.
532 Dedicated surveys and research on management practices effects are still
533 necessary in order to better estimate the reachable SOC stocks and the
534 feasibility of their implementation.

535 Further work will focus on estimating SOC storage potential by the model-
536 driven approach in mainland France. Producing model-driven estimates may
537 enable to determine a more reliable percentile setting for the data-driven
538 approach and thus provide references for the regions where exhaustive data
539 for applying process-based models is not available.

540 **Acknowledgement**

541 Soil data gathering was supported by a French Scientific Group of Interest on
542 soils: the GIS Sol, involving the French Ministry of Ecology, the French
543 Ministry of Agriculture, the French Environment and Energy Management
544 Agency (ADEME), the French Institute for Research and Development (IRD)
545 and the National Institute for Agronomic Research (INRA). We thank all the
546 people involved in sampling the sites and populating the database. Songchao
547 Chen received the support of China Scholarship Council for three years' Ph.D.

548 study in INRA and Agrocampus Ouest (under grant agreement no.
549 201606320211). This work will also constitute a main input to the ANR
550 (French Research National Agency) project StoreSoilC ANR-17-CE32-0005-
551 01.

552

553 **References**

554 Arrouays, D., Grundy, M.G., Hartemink, A.E., Hempel, J.W., Heuvelink, G.B.,
555 Young Hong, S., ... Zhang, G., 2014. GlobalSoilMap: Toward a fine-
556 resolution global grid of soil properties. *Adv. Agrono.* 125, 93-134.

557 Arrouays, D., Pélissier, P., 1994. Changes in carbon storage in temperate
558 humic loamy soils after forest clearing and continuous corn cropping in
559 France. *Plant Soil* 160, 215-223.

560 Arrouays, D., Balesdent, J., Mariotti, A., Girardin, C., 1995a. Modelling organic
561 carbon turnover in cleared temperate forest soils converted to maize
562 cropping by using ¹³C natural abundance measurements. *Plant Soil*
563 173(2), 191-196.

564 Arrouays, D., Vion, I., Kicin, J.L., 1995b. Spatial analysis and modeling of
565 topsoil carbon storage in forest humic loamy soils of France. *Soil Sci.* 159,
566 191-198.

567 Augusto, L., Bakker, M.R., Morel, C., Meredieu, C., Trichet, P., Badeau, V., ...
568 Ranger, J., 2010. Is grey literature a reliable source of data to characterize
569 soils at the scale of the region? A case study in a maritime pine forest of

570 south-western France. *Eur. J. Soil Sci.* 61, 807-822.

571 Barré, P., Angers, D. A., Basile-Doelsch, I., Bispo, A., Cécillon, L., Chenu,
572 C., ... Pellerin, S., 2017. Ideas and perspectives: Can we use the soil
573 carbon saturation deficit to quantitatively assess the soil carbon storage
574 potential, or should we explore other strategies?. *Biogeosciences Discuss.*
575 <https://doi.org/10.5194/bg-2017-395>.

576 Adair, E.C., Parton, W.J., Del Grosso, S.J., Silver, W.L., Harmon, M.E., Hall,
577 S.A., ... Hart, S.C., 2008. Simple three-pool model accurately describes
578 patterns of long-term litter decomposition in diverse climates. *Glob. Chang.*
579 *Bio.* 14(11), 2636-2660.

580 Chen, S., Martin, M.P., Saby, N.P., Walter, C., Angers, D.A., Arrouays, D.,
581 2018. Fine resolution map of top-and subsoil carbon sequestration
582 potential in France. *Sci. Total Environ.* 630, 389-400.

583 Chenu, C., Angers, D.A., Barré, P., Derrien, D., Arrouays, D., Balesdent, J.,
584 2018. Increasing organic stocks in agricultural soils: Knowledge gaps and
585 potential innovations. *Soil Till. Res.*
586 <https://doi.org/10.1016/j.still.2018.04.011>.

587 De Gruijter, J.J., Minasny, B., McBratney, A.B., 2015. Optimizing stratification
588 and allocation for design-based estimation of spatial means using
589 predictions with error. *J. Surv. Stat. Meth.* 3(1), 19-42.

590 Fick, S.E., Hijmans, R.J., 2017. WorldClim 2: new 1 km spatial resolution
591 climate surfaces for global land areas. *Int. J. Climatol.* 37(12), 4302-4315.

592 Hargreaves, G.H., Allen, R.G., 2003. History and evaluation of Hargreaves
593 evapotranspiration equation. *J. Irrig. Drain. E.* 129, 53–63.

594 Hargreaves, G.L., Hargreaves, G.H., Riley, J.P., 1985. Irrigation water
595 requirements for Senegal River Basin. *J. Irrig. Drain. E.* 111, 265–275.

596 Hassink, J., 1997. The capacity of soils to preserve organic C and N by their
597 association with clay and silt particles. *Plant Soil*, 191(1), 77-87.

598 Lacoste, M., Mulder, V.L., Richer-de-Forges, A.C., Martin, M.P., Arrouays, D.,
599 2016. Evaluating large-extent spatial modelling approaches: a case study
600 for soil depth for France. *Geoderma Regional*, 7, 137-152.

601 Lal, R., Negassa, W., Lorenz, K., 2015. Carbon sequestration in soil. *Curr.*
602 *Opin. Env. Sust.* 15, 79–86.

603 Lal, R., 2004. Soil carbon sequestration impacts on global climate change and
604 food security. *Science*, 304, 1623-1627.

605 Lal, R., 2016. Beyond COP 21: potential and challenges of the “4 per
606 Thousand” initiative. *J. Soil Water Conserv.* 71(1), 20A-25A.

607 Lilly, A., Baggaley, N.J., 2013. The potential for Scottish cultivated topsoils to
608 lose or gain soil organic carbon. *Soil Use Manag.* 29, 39-47.

609 Lugato, E., Bampa, F., Panagos, P., Montanarella, L., Jones, A., 2014.
610 Potential carbon sequestration of European arable soils estimated by
611 modelling a comprehensive set of management practices. *Glob. Chang.*
612 *Biol.* 20(11), 3557-3567.

613 Martin, M.P., Lo Seen, D., Boulonne, L., Jolivet, C., Nair, K.M., Bourgeon, G.,

614 Arrouays, D., 2009. Optimizing pedotransfer functions for estimating soil
615 bulk density using boosted regression trees. *Soil Sci. Soc. Am.J.* 73(2),
616 485-493.

617 Martin, M.P., Orton, T.G., Lacarce, E., Meersmans, J., Saby, N.P.A.,
618 Paroissien, J.B., ... Arrouays, D., 2014. Evaluation of modelling
619 approaches for predicting the spatial distribution of soil organic carbon
620 stocks at the national scale. *Geoderma*, 223, 97–107.

621 Minasny, B., Malone, B.P., McBratney, A.B., Angers, D.A., Arrouays, D.,
622 Chambers, A., ... Winowiecki, L., 2017. Soil carbon 4 per mille. *Geoderma*,
623 292, 59-86.

624 Mouselimis, L. 2016. Clustering using the ClusterR package.
625 http://mlampros.github.io/2016/09/12/clusterR_package/

626 Mulder, V.L., Lacoste, M., Martin, M.P., Richer-de-Forges, A. and Arrouays,
627 D., 2015. Understanding large-scale controls of soil organic carbon
628 storage in relation to soil depth and soil-landscape systems. *Glob.*
629 *Biogeochem. Cycles* 29, 1210–1229.

630 Mulder, V.L., Lacoste, M., Richer-de-Forges, A.C. and Arrouays, D., 2016.
631 GlobalSoilMap France: High-resolution spatial modelling the soils of
632 France up to two meter depth. *Sci. Total Environ.* 573, 1352-1369.

633 NASA LP DAAC, 2017. MOD17A2H: MODIS/TERRA Gross Primary
634 Production. Version 6. NASA EOSDIS Land Processes DAAC, USGS
635 Earth Resources Observation and Science (EROS) Center, Sioux Falls,

636 South Dakota (<https://lpdaac.usgs.gov>), accessed October 30, 2017, at
637 <http://dx.doi.org/10.5067/MODIS/MOD17A2H.006>.

638 Paustian, K., Lehmann, J., Ogle, S., Reay, D., Robertson, G.P., Smith, P.,
639 2016. Climate-smart soils. *Nature*, 532, 49.

640 Post, W.M., Kwon, K.C., 2000. Soil carbon sequestration and land use
641 change: processes and potential. *Glob. Chang. Biol.* 6(3), 317-327.

642 R Core Team, 2016. R: A language and environment for statistical computing.
643 R Foundation for Statistical Computing, Vienna, Austria. URL
644 <https://www.R-project.org/>.

645 Saby, N.P.A., Arrouays, D., Antoni, V., Foucaud-lemercier, B., Follain, S.,
646 Walter, C., Schwartz, C., 2008. Changes in soil organic carbon content in
647 a French mountainous region, 1990-2004. *Soil Use Manag.* 24, 254-262.

648 Sanchez, P.A., Ahamed, S., Carre, F., Hartemink, A.E., Hempel, J., Huising,
649 J., ... Zhang, G.L., 2009. Digital soil map of the world. *Science*, 325, 680–
650 681.

651 Six, J., Conant, R.T., Paul, E.A., Paustian, K., 2002. Stabilization mechanisms
652 of soil organic matter: implications for C-saturation of soils. *Plant Soil*,
653 241(2), 155-176.

654 Sparling, G., Parfitt, R.L., Hewitt, A.E., Schipper, L.A., 2003. Three
655 approaches to define desired soil organic matter content. *J. Environ. Qual.*
656 32, 760-766.

657 Stockmann, U., Adams, M., Crawford, J.W., Field, D.J., Henakaarchchi, N.,

658 Jenkins, M., ... Zimmermann, M., 2013. The knowns, known unknowns
659 and unknowns of sequestration of soil organic carbon. *Agr. Ecosyst.*
660 *Environ.* 164, 80-99.

661 Stolbovoy, V., Montanarella, L., 2008. Application of soil organic carbon status
662 indicators for policy-decision making in the EU, In: Toth, G., Montanarella,
663 L., Rusco, E. (Eds.), *Threats to soil quality in Europe*, 87–99.

664 UE-SOeS (2006) Corine Land Cover. Service de l'Observation et des
665 Statistiques (SOeS) du Ministère de l'Environnement. de l'Énergie et de la
666 Mer. Tech. rep.

667

668 **Figure captions**

669 Figure 1 RMQS sites located in arable soils.

670 Figure 2 Spatial distribution of monthly climatic decomposition index and net
671 primary production. X and Y coordinates are expressed in Lambert 93
672 projection.

673 Figure 3 Spatial distribution of principal components for climatic
674 decomposition index and net primary production.

675 Figure 4 Relationship between the number of clusters and BIC.

676 Figure 5 Number of RMQS sites located in each carbon-landscape zone.

677 Figure 6 Optimal 10 carbon-landscape zones in France.

678 Figure 7 Boxplots of SOC content in topsoil and subsoil under 10 carbon-
679 landscape zones.

680 Figure 8 Empirically maximum SOC stocks in topsoil and subsoil under four
681 percentile settings. The four colours are related to four percentiles. For each
682 percentile, bar shows the interval between upper limit and lower limit of 90%
683 CIs. Number of samples is shown in grey.

684 Figure 9 SOC storage potential for arable topsoil under four percentile
685 settings.

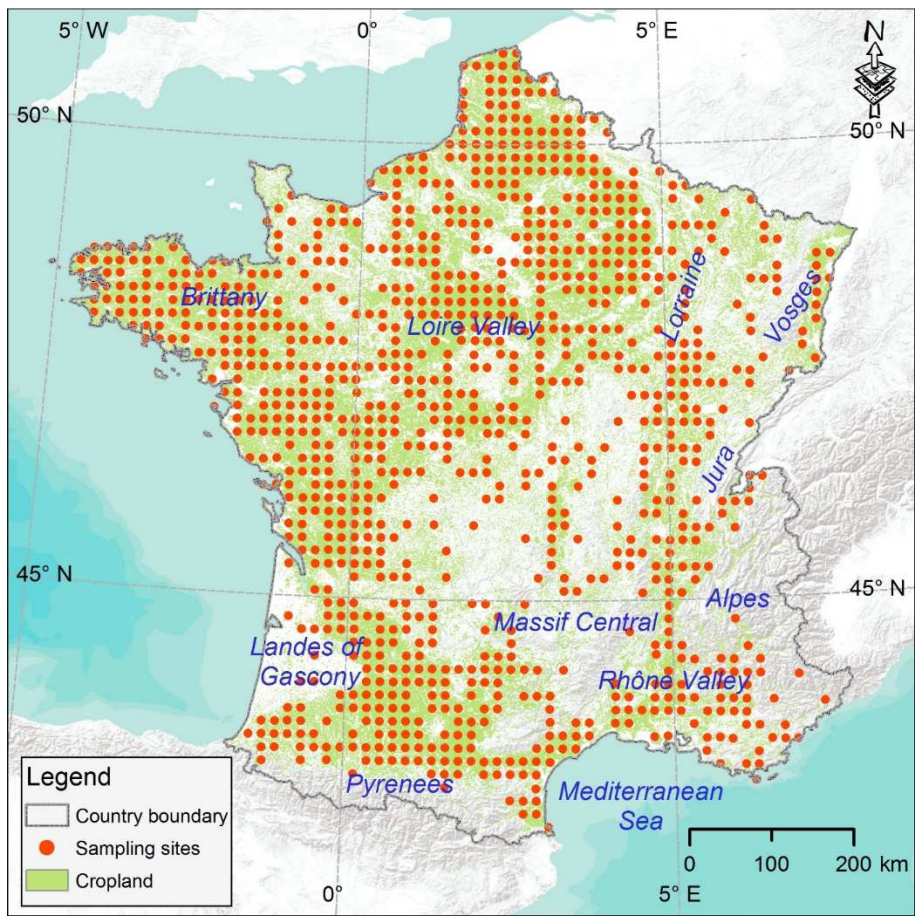
686 Figure 10 SOC storage potential for arable subsoil under four percentile
687 settings.

688 **Table captions**

689 Table 1 National SOC storage potential stocks of French arable soils under
690 different percentile settings. Lower limit and upper limit of 90% CIs are also
691 provided.

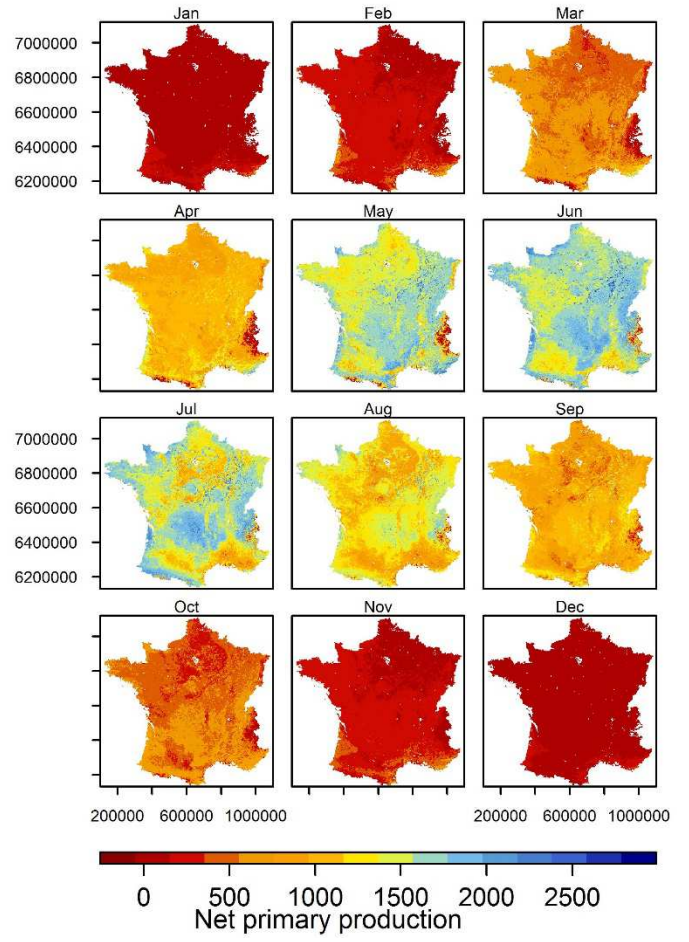
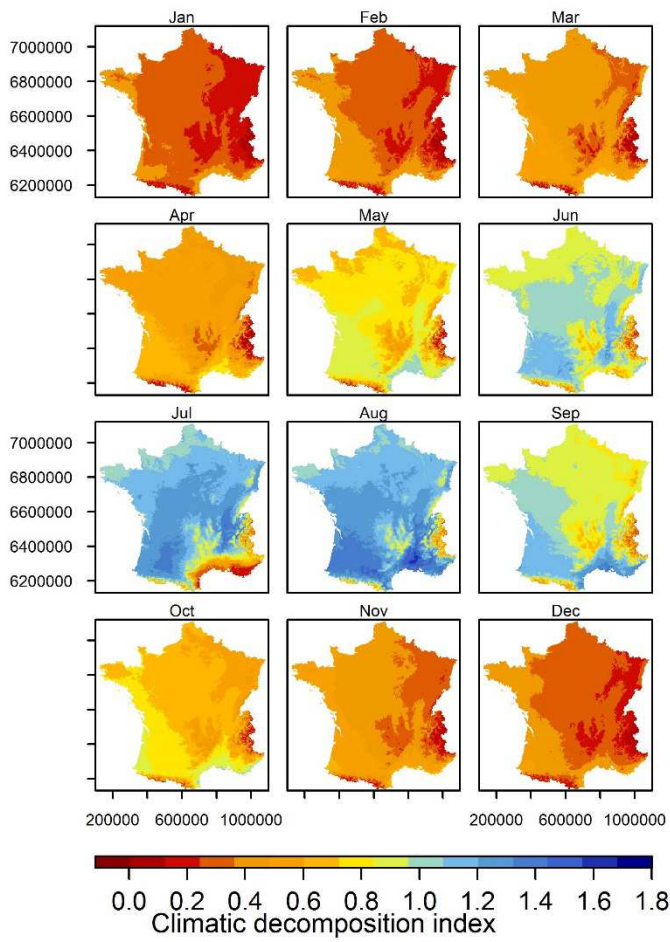
692

693 Figure 1

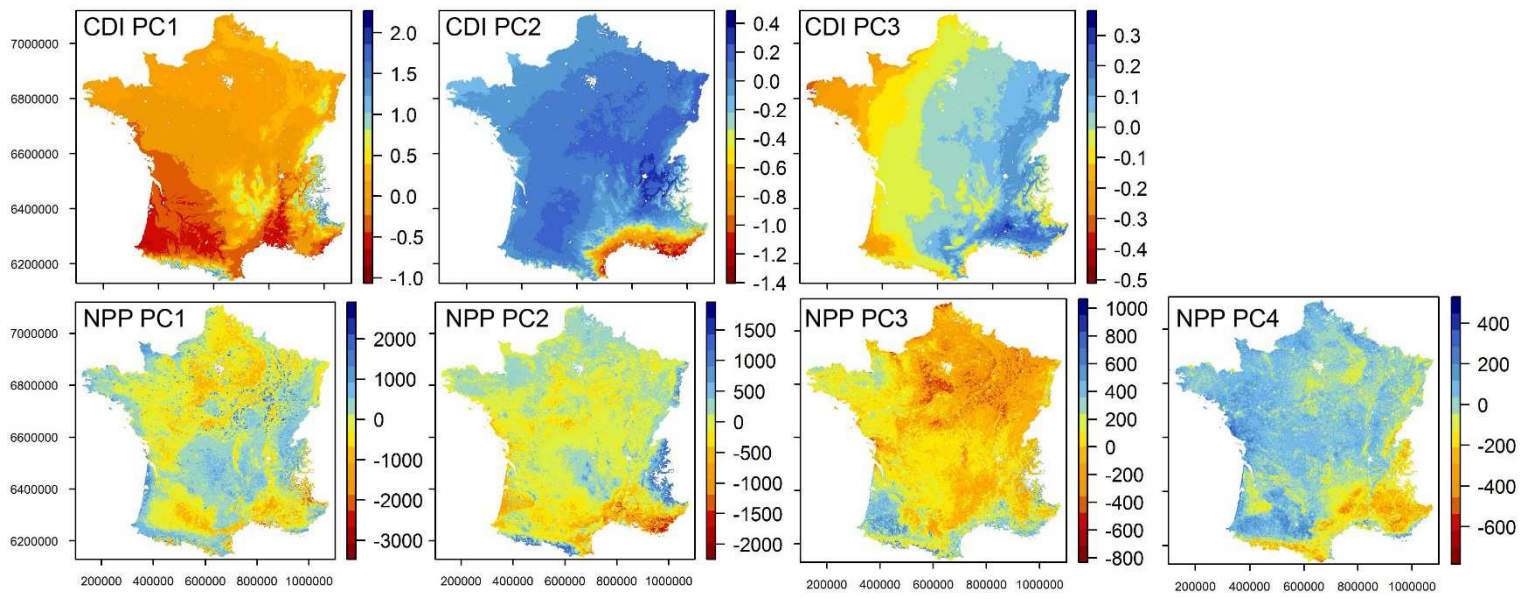


694

695 Figure 2

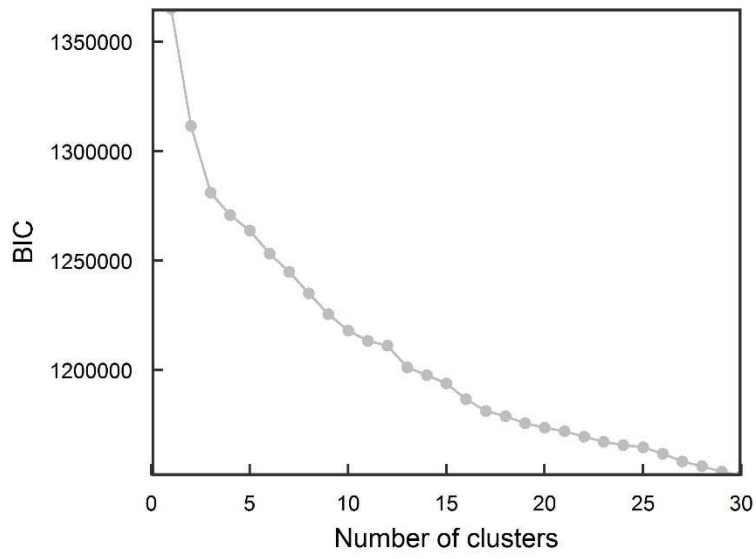


697 Figure 3



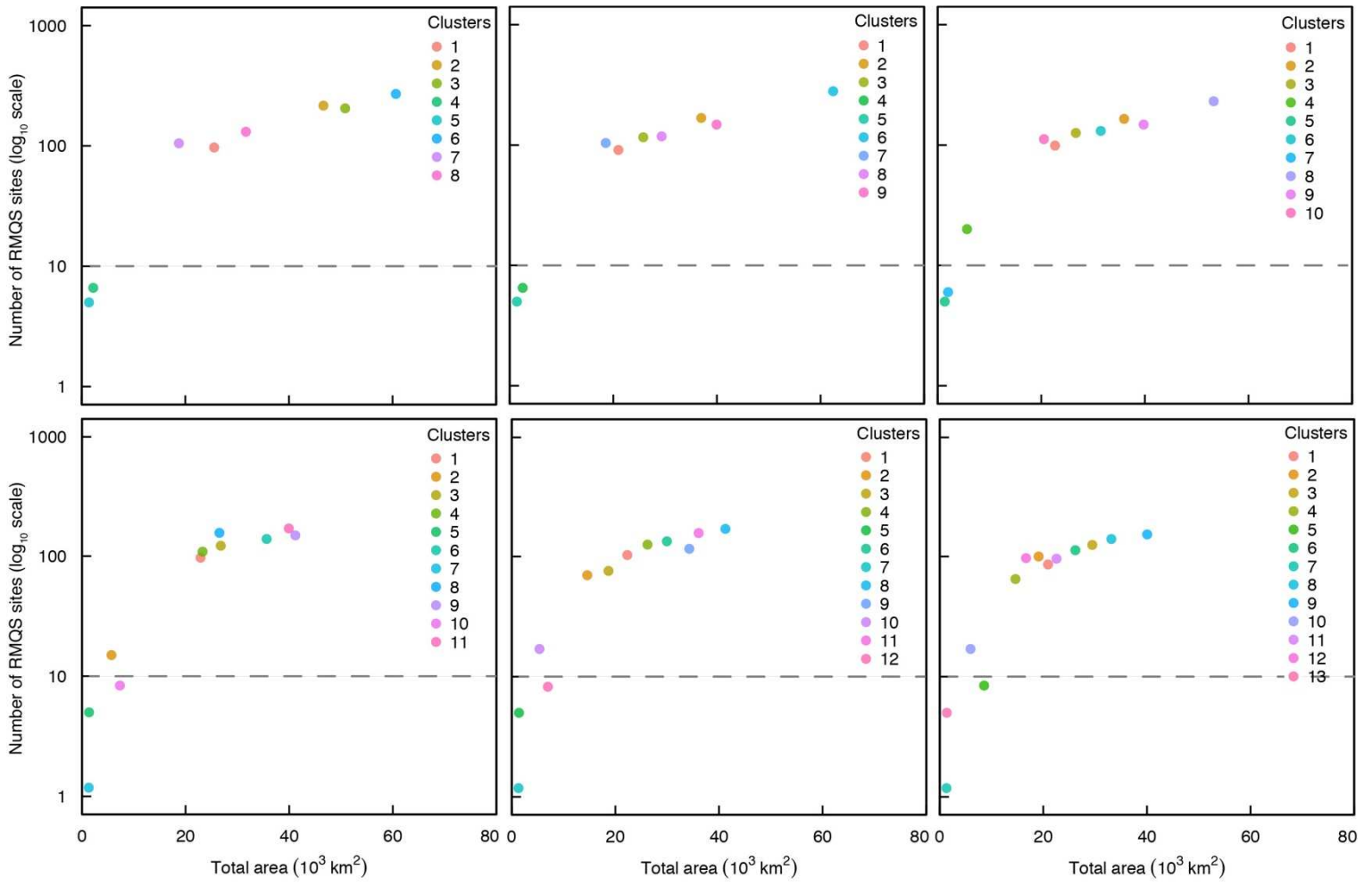
698

699 Figure 4

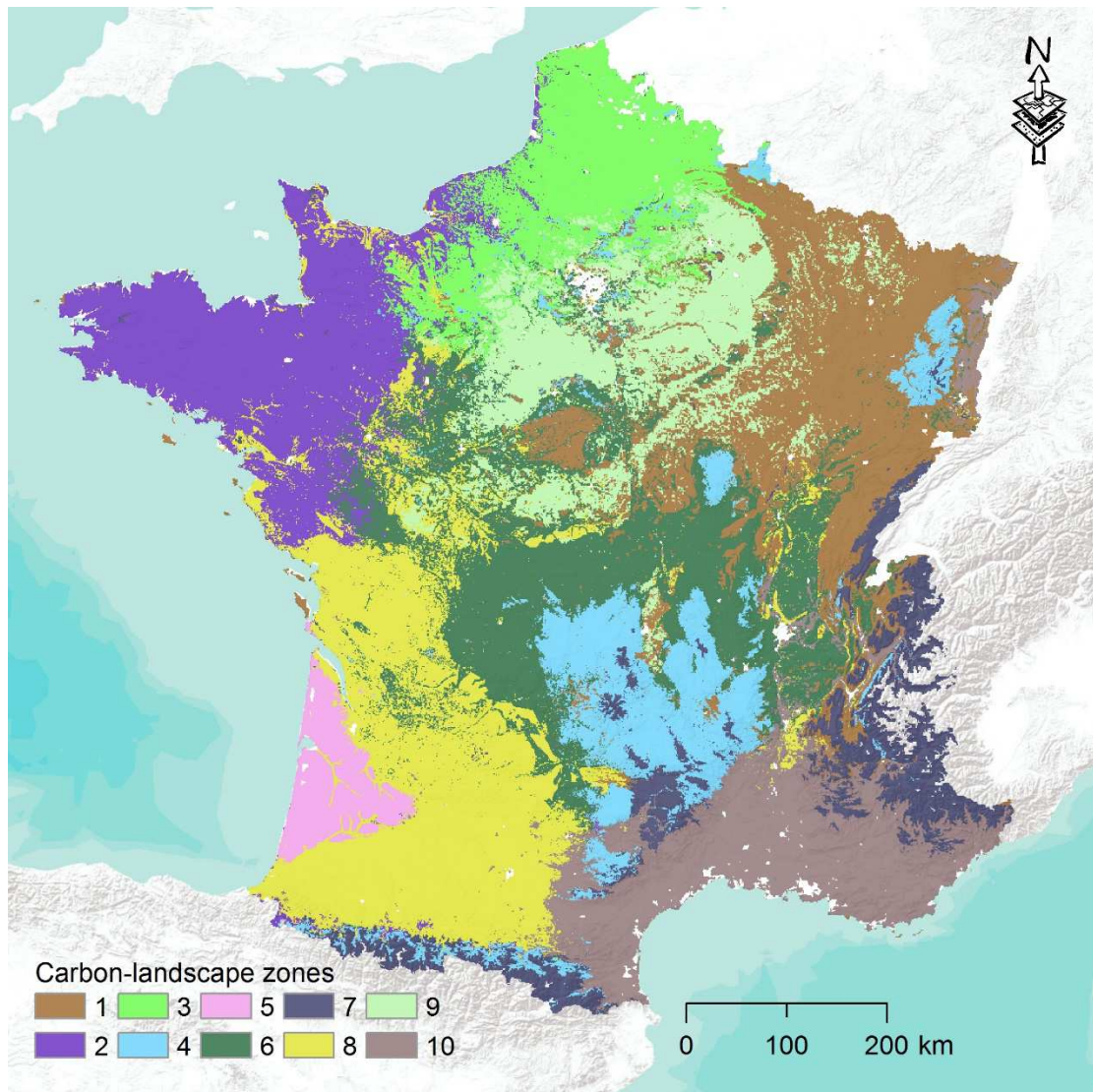


700

701



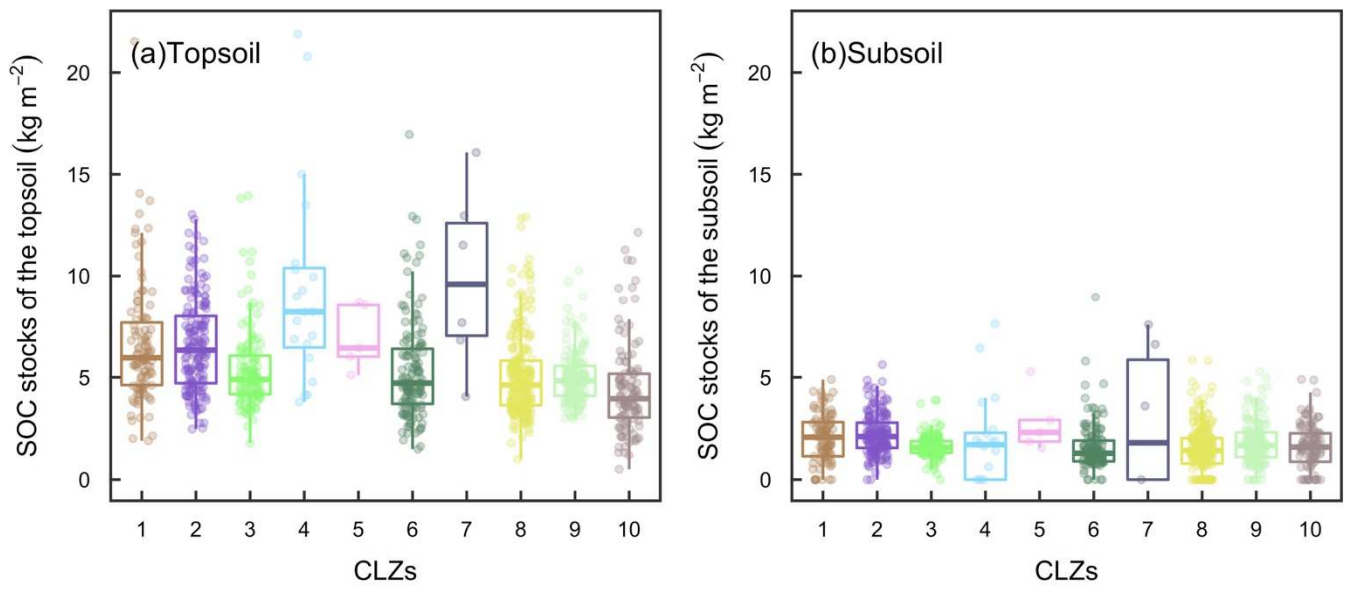
704 Figure 6



705

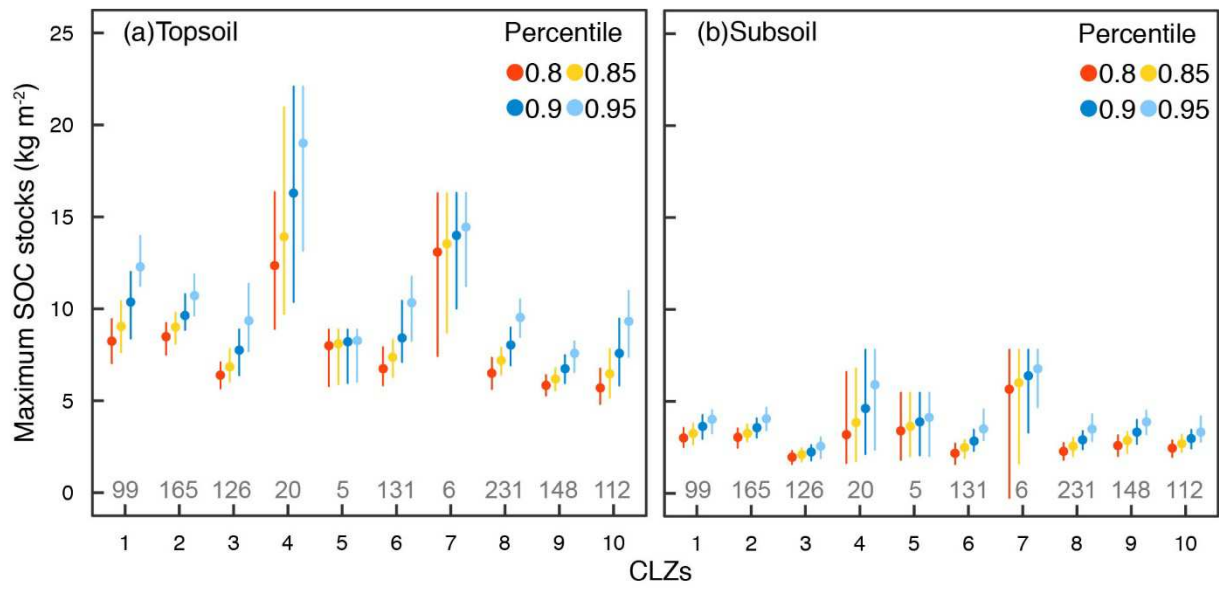
706

707 Figure 7



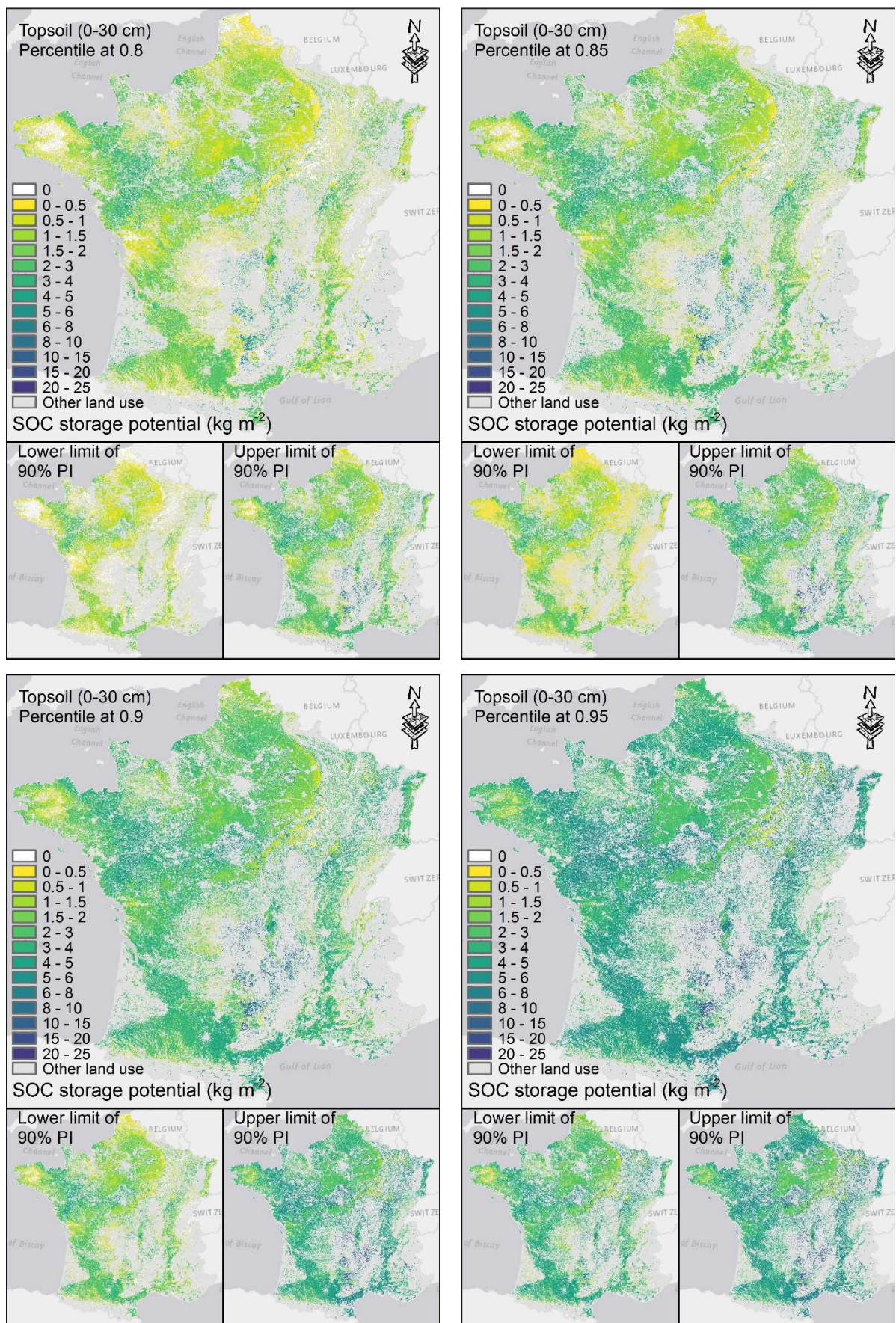
708

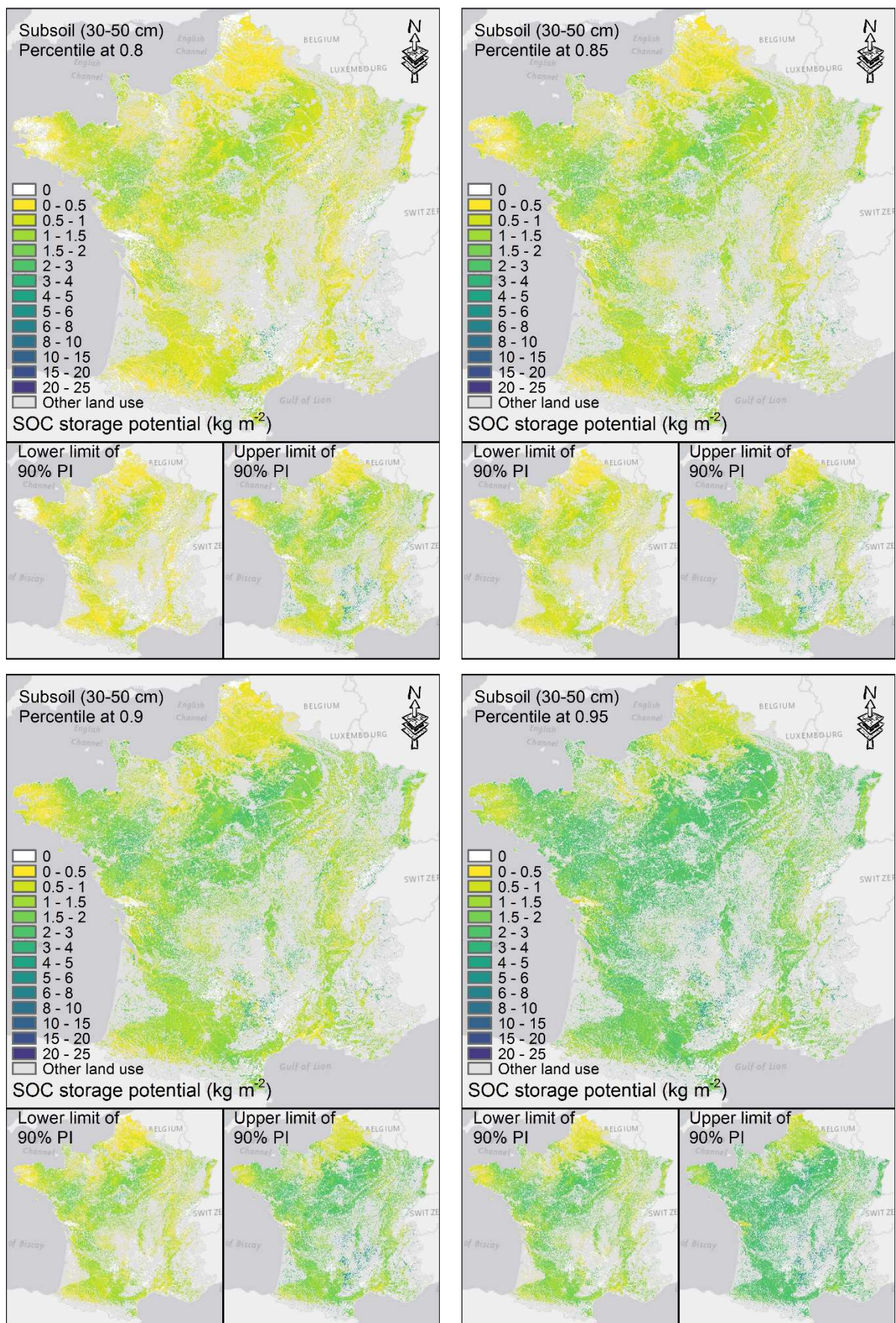
709 Figure 8



710

711 Figure 9





713 Table 1

Soil horizon	Area (km ²)	Total SOC storage potential under four percentile settings (Mt)			
		0.8	0.85	0.9	0.95
Topsoil	239395	336(203,501)	470(308,662)	674(434,950)	1020(740,1283)
Subsoil	228467	165(91,250)	228(150,306)	309(226,404)	433(331,560)

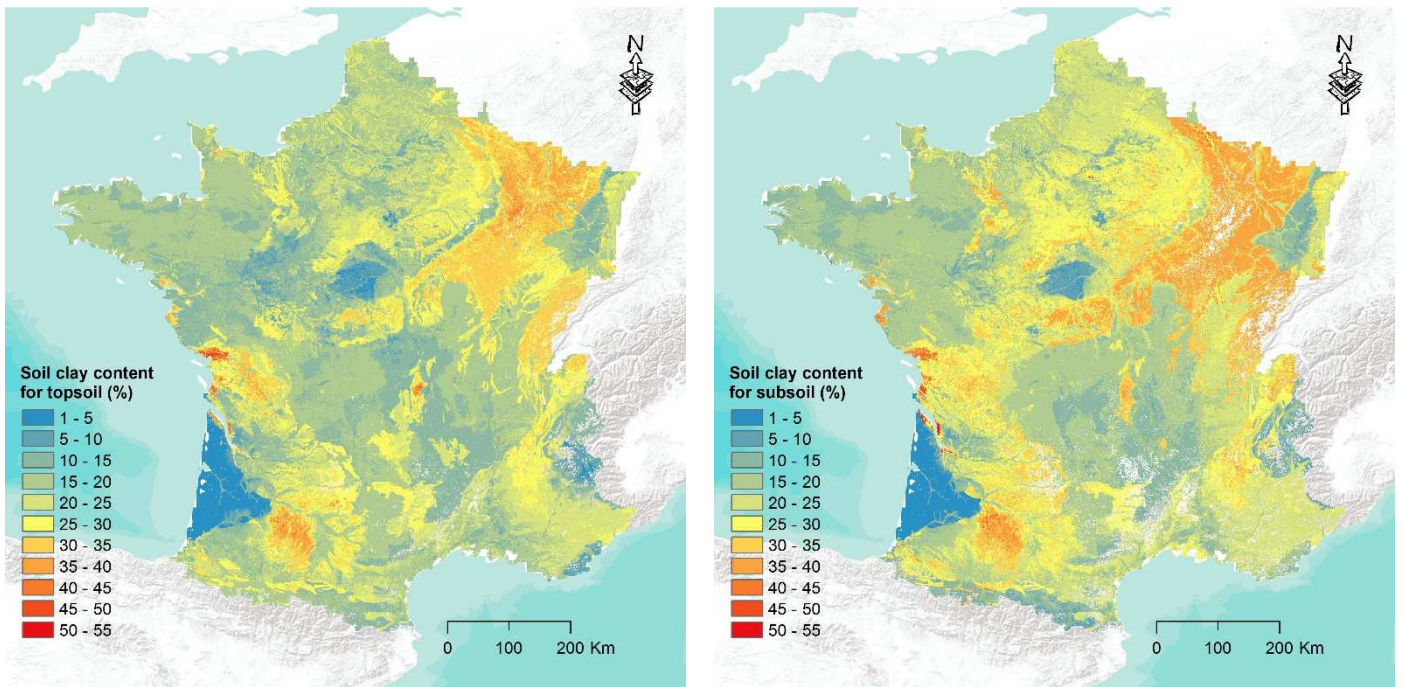


Figure A1 Soil clay content for topsoil and subsoil

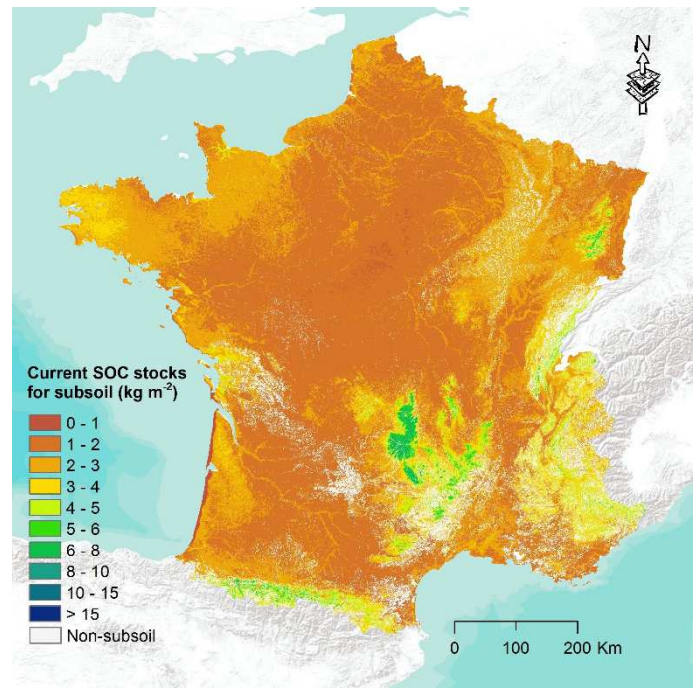
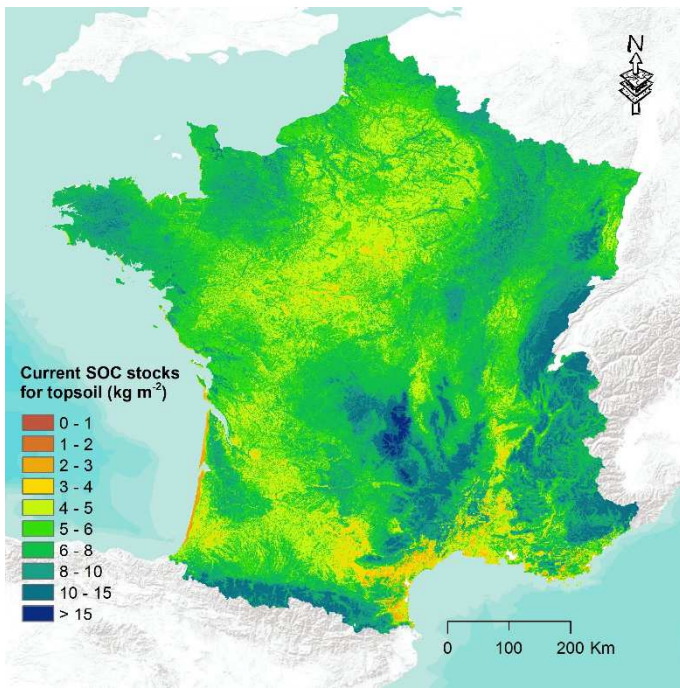


Figure A2 Current SOC stocks for topsoil and subsoil

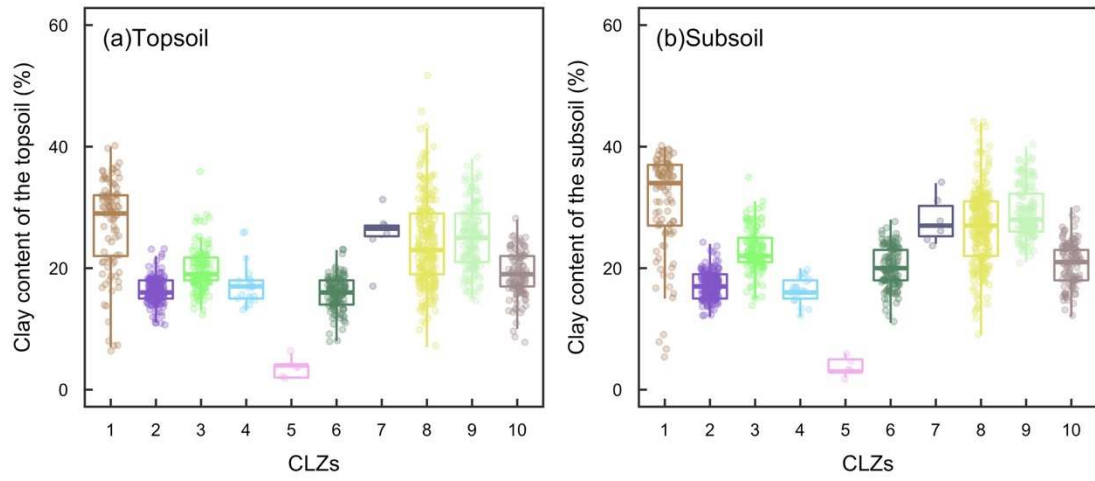
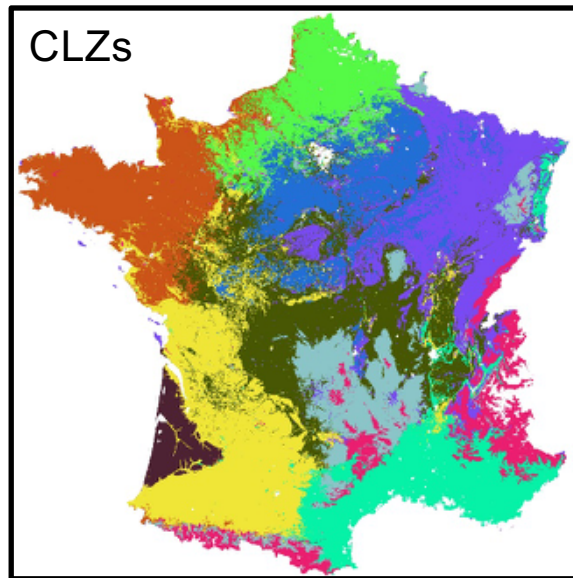
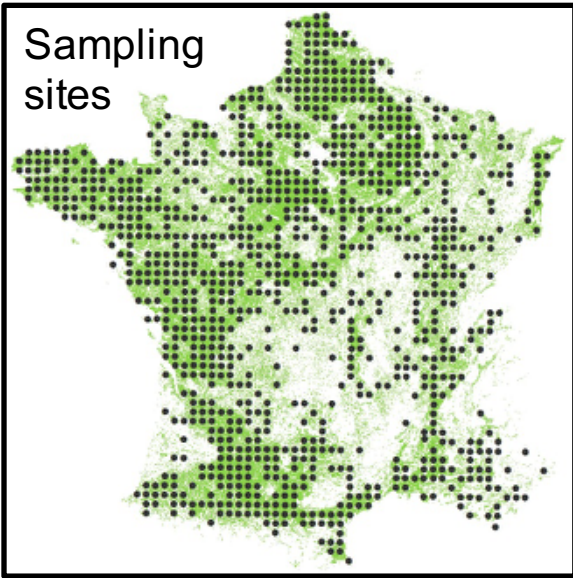
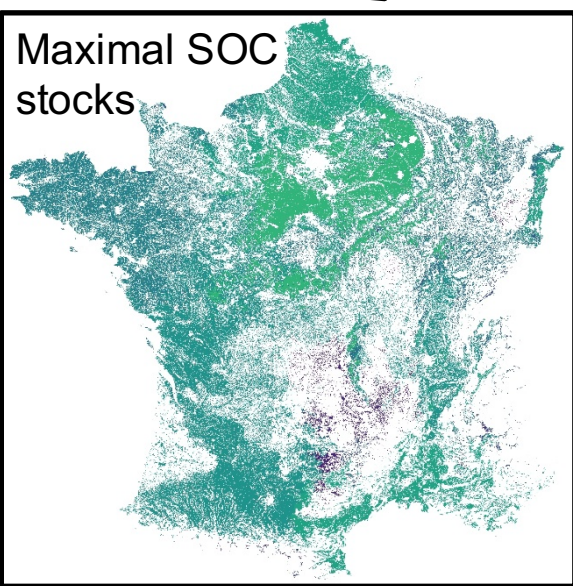
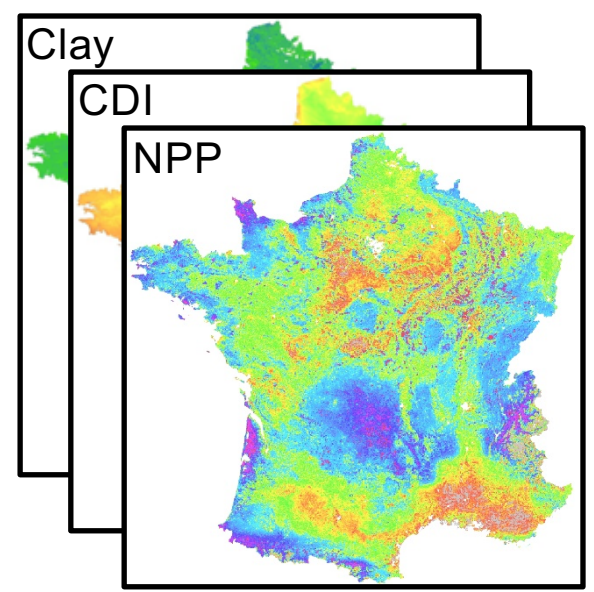


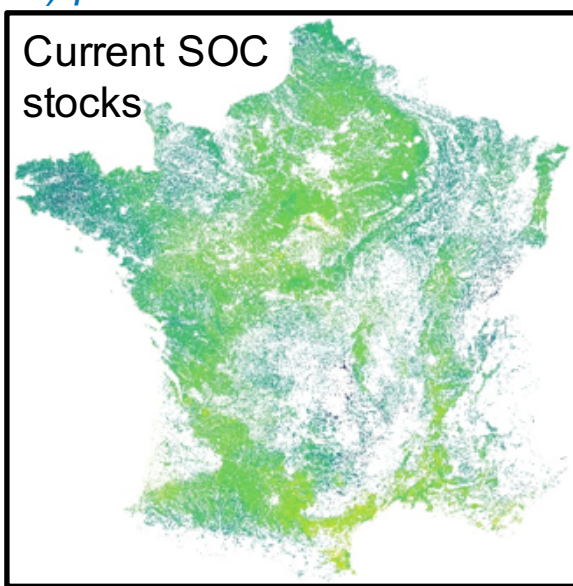
Figure A3 Boxplots of clay content in topsoil and subsoil under the 10 carbon-landscape zones.



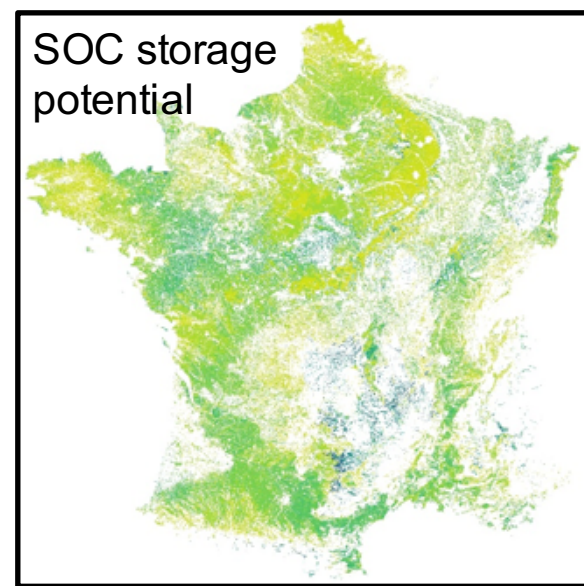
Clustering
←



Determine maximal SOC by four percentiles (0.8, 0.85, 0.9, 0.95) per each CLZ



Minus
→



CLZs, carbon-landscape zones; CDI, climatic decomposition index; NPP, net primary production.